Phys. Lett. B 848 (2024) 138395

Contents lists available at ScienceDirect

Physics Letters B

journal homepage: www.elsevier.com/locate/physletb

Letter

Extraction of kaon partonic distribution functions from Drell-Yan and J/ψ production data

Claude Bourrely [a,*], Franco Buccella [b], Wen-Chen Chang [c], Jen-Chieh Peng [d]

[a] Aix Marseille Univ, Universite de Toulon, CNRS, CPT, Marseille, France
[b] INFN, Sezione di Roma I, Roma, Italy
[c] Institute of Physics, Academia Sinica, Taipei 11529, Taiwan
[d] Department of Physics, University of Illinois at Urbana-Champaign, Urbana, IL 61801, USA

ARTICLE INFO

Editor: G.F. Giudice

ABSTRACT

We present an analysis to extract kaon parton distribution functions (PDFs) using meson-induced Drell-Yan and quarkonium production data. Starting from the statistical model first developed for determining the partonic structure of spin-1/2 nucleon and later applied to the spin-0 pion, we have extended this approach to perform a global fit to existing kaon-induced Drell-Yan and J/ψ production data. These data are well described by the statistical model, allowing an extraction of the kaon PDFs. We find that both the Drell-Yan and the J/ψ data favor a harder valence distribution for strange quark than for up quark in kaon. The kaon gluon distribution is further constrained by the J/ψ production data. In particular, the momentum fraction carried by gluons is found to be similar for pion and kaon.

The study of proton's partonic substructure has been actively pursued since the discovery of point-like constituents of the nucleons in deep-inelastic scattering (DIS) reaction. In contrast, the partonic substructures of pion and kaon, which are the lightest hadrons with the dual roles of $q\bar{q}$ bound states and Goldstone bosons, remain poorly studied experimentally [1]. The lack of DIS data on these ephemeral particles represents a major limitation for accessing their substructures experimentally. Nevertheless, pion-induced Drell-Yan process [2] has provided a first glimpse of the valence-quark distribution in pion [3–5]. These data, together with the pion-induced direct-photon production and the tagged-neutron DIS data, have led to the extraction of parton distributions in pion [6–11], although the sea-quark and gluon distributions remain to be better determined. It was pointed out [12–15] that pion-induced J/ψ production data could probe the gluon as well as the valence-quark distributions in pion.

Compared to the situation for proton and pion, extremely limited information on the partonic structure of kaon is available experimentally. Based on a total of ~ 700 Drell-Yan events using a K^- beam [16], the NA3 collaboration inferred that the $\bar{u}$ valence quark in K^- has a softer momentum distribution than that in π^-. This reflects the breaking of the SU(3) flavor symmetry, resulting in a larger fraction of K^-'s momentum being carried by the s quarks than the lighter $\bar{u}$ quarks. The indication of a flavor dependence of valence-quark distributions in kaon has generated much interest, and has inspired many theoretical calculations [17–22]. Recent advent in lattice QCD to calculate the momentum (x) dependence of meson parton distribution functions (PDFs) [23–30] as well as the suggestion that the gluon content of kaon is different from that of pion [18], has led to new initiatives for collecting additional Drell-Yan data with kaon beams [31].

While several sets of pion PDFs have been obtained from global analyses of existing data, the kaon PDFs have only been extracted based on a fit to the scarce NA3 K^-/π^- Drell-Yan data. It was suggested that the more abundant kaon-induced J/ψ production data could constrain the kaon PDFs [12]. Indeed, pion-induced J/ψ production data, together with the Drell-Yan data, were included in a recent global fit to extract the pion PDFs in the framework of a statistical model [32]. This paper reports the extraction of the kaon PDFs from a global fit to the kaon-induced Drell-Yan and J/ψ production data in the statistical model.

The statistical approach for describing the partonic distributions in hadrons was initiated over 20 years ago [33]. Valuable insights on the flavor and spin structure of the momentum dependencies of quarks and gluons in the proton have been provided with the statistical model [34]. A salient feature of the statistical model is the connection between the valence and the sea quark distributions through their

* Corresponding author.
E-mail addresses: claude.bourrely@cpt.univ-mrs.fr, crv.bourrely@orange.fr (C. Bourrely).

https://doi.org/10.1016/j.physletb.2023.138395
Received 24 September 2023; Received in revised form 2 December 2023; Accepted 7 December 2023
Available online 12 December 2023

helicity-dependent Fermi-Dirac momentum distributions. The statistical model approach has led to many successful predictions [34], including the flavor asymmetry, $\bar{d}(x) > \bar{u}(x)$, for the unpolarized sea [35–37] and the inequality, $\Delta\bar{u}(x) > 0 > \Delta\bar{d}(x)$, for the polarized sea [38]. As discussed in a review of major results obtained in the statistical model approach, the collider data on jet and W-boson production at Tevatron, RHIC, and LHC are also very well described by calculations based on proton parton distributions deduced from the statistical model [39].

To extract the kaon PDFs in the statistical model, we first define the notations of the PDFs of pions and kaons. Imposing the particle-antiparticle charge-conjugation (C) symmetry and the isospin symmetry for parton distributions [40], we can define the PDFs of charged pions as follows [44]:

$$\begin{aligned}
U_\pi(x) &\equiv u_{\pi^+}(x) = \bar{u}_{\pi^-}(x) = \bar{d}_{\pi^+}(x) = d_{\pi^-}(x)\ ;\\
\bar{U}_\pi(x) &\equiv \bar{u}_{\pi^+}(x) = \bar{d}_{\pi^-}(x) = d_{\pi^+}(x) = u_{\pi^-}(x)\ ;\\
S_\pi(x) &\equiv s_{\pi^+}(x) = \bar{s}_{\pi^-}(x) = \bar{s}_{\pi^+}(x) = s_{\pi^-}(x)\ ;\\
G_\pi(x) &\equiv g_{\pi^+}(x) = g_{\pi^-}(x)\ . \qquad (1)
\end{aligned}$$

In the framework of the statistical model, the four pion parton distributions are given in the following parametric forms [32]:

$$\begin{aligned}
xU_\pi(x) &= \frac{A_U X_U x^{b_U}}{\exp[(x-X_U)/\bar{x}]+1} + \frac{\tilde{A}_U x^{\tilde{b}_U}}{\exp(x/\bar{x})+1}\ ;\\
x\bar{U}_\pi(x) &= \frac{A_U (X_U)^{-1} x^{b_U}}{\exp[(x+X_U)/\bar{x}]+1} + \frac{\tilde{A}_U x^{\tilde{b}_U}}{\exp(x/\bar{x})+1}\ ;\\
xS_\pi(x) &= \frac{\tilde{A}_U x^{\tilde{b}_U}}{2[\exp(x/\bar{x})+1]}\ ;\\
xG_\pi(x) &= \frac{A_G x^{b_G}}{\exp(x/\bar{x})-1}\ , \quad b_G = 1+\tilde{b}_U\ . \qquad (2)
\end{aligned}$$

The x distributions for quarks and antiquarks have Fermi-Dirac parametric form, while gluon has a Bose-Einstein form [33,34]. The two terms in $xU_\pi(x)$ and $x\bar{U}_\pi(x)$ correspond to the non-diffractive and diffractive contributions [33,34]. As shown in [34], the diffractive term is important at the low x region. A key feature of the statistical model is that the chemical potential, X_U, for the parton distribution becomes $-X_U$ for the anti-parton distribution. The parameter $\bar{x}$ signifies the effective "temperature". For the strange-quark distribution, $S_\pi(x)$, the absence of the valence strange quarks implies that the chemical potential must vanish for the non-diffractive term. The assumption that $S_\pi(x)$ equals half of the diffractive part of $\bar{U}_\pi(x)$ reflects the heavier strange quark mass. The expression $b_G = 1+\tilde{b}_U$ ensures that $G(x)$ has an identical x dependence as the diffractive part of the quark distributions when $x \to 0$.

For charged kaons, as K^+ and K^- belong to different isospin multiplets, only the charge-conjugation symmetry is applicable. The kaon PDFs are then defined as:

$$\begin{aligned}
U_K(x) &\equiv u_{K^+}(x) = \bar{u}_{K^-}(x)\ ;\\
S_K(x) &\equiv \bar{s}_{K^+}(x) = s_{K^-}(x)\ ;\\
D_K(x) &\equiv d_{K^+}(x) = \bar{d}_{K^-}(x)\ ;\\
G_K(x) &\equiv g_{K^+}(x) = g_{K^-}(x)\ , \qquad (3)
\end{aligned}$$

with analogous expressions for $\bar{U}_K(x), \bar{S}_K(x)$ and $\bar{D}_K(x)$. The kaon PDFs are constrained by the valence-quark and the momentum sum rule:

$$\begin{aligned}
&\int_0^1 [U_K(x) - \bar{U}_K(x)]\, dx = 1\ ,\\
&\int_0^1 [S_K(x) - \bar{S}_K(x)]\, dx = 1\ ,\\
&\int_0^1 x[U_K(x) + \bar{U}_K(x) + S_K(x) + \bar{S}_K(x) +\\
&\qquad 2D_K(x) + G_K(x)]\, dx = 1\ . \qquad (4)
\end{aligned}$$

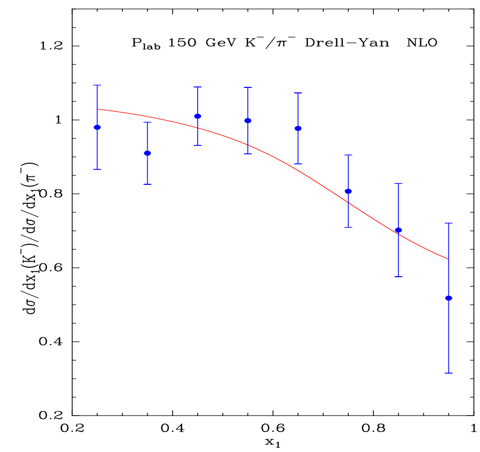

Fig. 1. K^-/π^- Drell-Yan cross section ratio data from the NA3 experiment at beam momentum of 150 GeV on a platinum target [16]. The data are compared with NLO calculation using the kaon PDFs obtained in this analysis and the pion PDFs obtained in a recent analysis [32] using the statistical model.

The kaon parton distributions in the statistical model are expressed in the following parametric forms:

$$\begin{aligned}
xU_K(x) &= \frac{A_{UK} X_{UK} x^{b_{UK}}}{\exp[(x-X_{UK})/\bar{x}]+1} + \frac{\tilde{A}_{UK} x^{\tilde{b}_{UK}}}{\exp(x/\bar{x})+1}\ ;\\
x\bar{U}_K(x) &= \frac{A_{UK} (X_{UK})^{-1} x^{b_{UK}}}{\exp[(x+X_{UK})/\bar{x}]+1} + \frac{\tilde{A}_{UK} x^{\tilde{b}_{UK}}}{\exp(x/\bar{x})+1}\ ;\\
xS_K(x) &= \frac{A_{SK} X_{SK} x^{b_{SK}}}{\exp[(x-X_{SK})/\bar{x}]+1} + \frac{\tilde{A}_{UK} x^{\tilde{b}_{UK}}}{2[\exp(x/\bar{x})+1]}\ ;\\
x\bar{S}_K(x) &= \frac{A_{SK} (X_{SK})^{-1} x^{b_{SK}}}{\exp[(x+X_{SK})/\bar{x}]+1} + \frac{\tilde{A}_{UK} x^{\tilde{b}_{UK}}}{2[\exp(x/\bar{x})+1]}\ ;\\
xD_K(x) &= x\bar{D}_K(x) = \frac{\tilde{A}_{UK} x^{\tilde{b}_{UK}}}{(\exp(x/\bar{x})+1)}\ ;\\
xG_K(x) &= \frac{A_{GK} x^{b_{GK}}}{\exp(x/\bar{x})-1}\ , \quad b_{GK} = 1+\tilde{b}_{UK}\ . \qquad (5)
\end{aligned}$$

To obtain the parameters for kaon PDFs, we have fitted both the Drell-Yan and the J/ψ production data. The only available Drell-Yan data with kaon beam are from the NA3 collaboration, which performed a simultaneous measurement of $K^- +$ Pt $\to \mu^+\mu^- + X$ and $\pi^- +$ Pt $\to \mu^+\mu^- + X$ using a 150 GeV beam on a platinum target [16]. Fig. 1 shows the K^-/π^- Drell-Yan cross section ratios from NA3 as a function of x_1, the fraction of the beam momentum carried by the interacting parton. Fig. 1 shows that the ratio R falls below unity at large x_1 ($x_1 > 0.65$). Since the Drell-Yan cross sections with π^- and K^- beams at large x_1 are dominated by the term containing the product of $\bar{u}_M(x_1)$ in the meson M and $u_A(x_2)$ in the nucleus A, the fall-off in R at large x_1 indicates that $U_K(x)$ is softer than $U_\pi(x)$ [16].

We have performed a next-to-leading-order (NLO) QCD calculation to fit the NA3 K^-/π^- Drell-Yan data. Detailed expressions for the NLO Drell-Yan cross sections can be found in [41]. The nucleon PDFs used in the calculation were taken from the BS15 PDFs [39], obtained from a global fit to existing data in the framework of the statistical model. The QCD evolution was performed using the HOPPET program [42], and the CERN MINUIT program [43] was utilized for the χ^2 minimization. Since the NA3 Drell-Yan data were collected using nuclear targets (platinum), we take into account the nuclear modification of the nucleon PDFs, described in [44].

The NA3 collaboration also reported the measurement of K^-/π^- ratio versus x_F (x-Feynman) for J/ψ production at 150 GeV on a platinum target, shown in Fig. 2(a) [45]. While the K^-/π^- ratio is relatively flat for the region $0 < x_F < 0.6$, it starts to drop noticeably

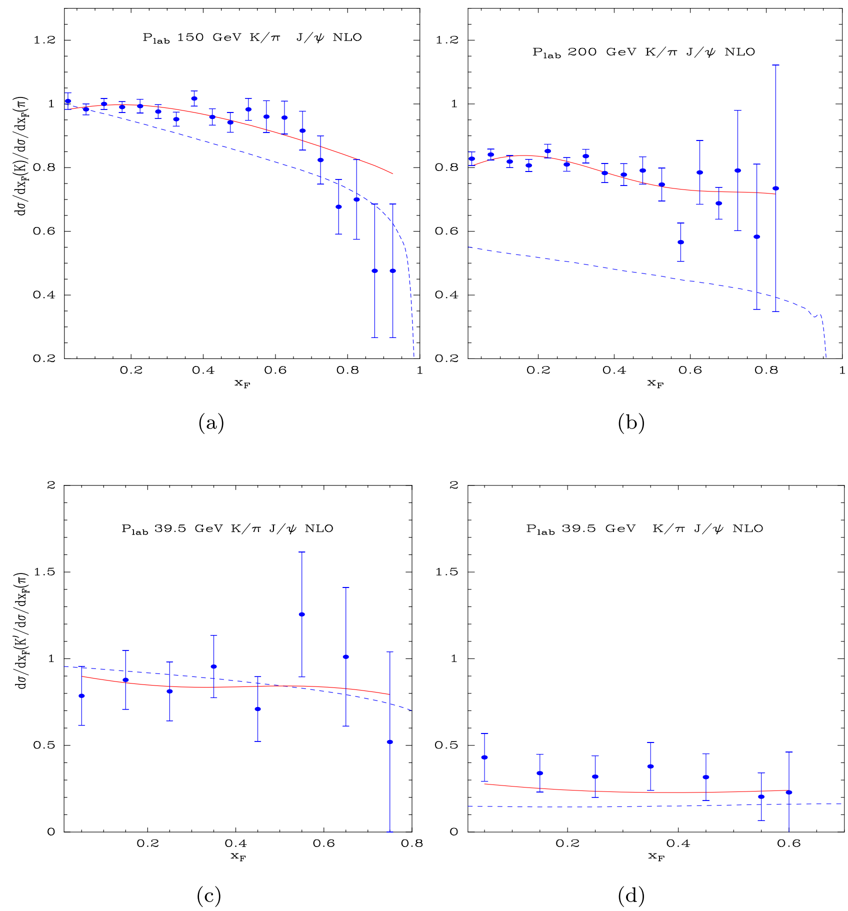

Fig. 2. J/ψ cross section ratios data on platinum targets for (a) K^-/π^- at 150 GeV [45], (b) K^+/π^+ at 200 GeV [45], (c) K^-/π^- at 39.5 GeV [46], and (d) K^+/π^+ at 39.5 GeV [46]. The solid curves are NRQCD calculation using the kaon and pion PDFs obtained in the statistical model, while the dashed curves correspond to NRQCD calculation using the meson PDFs from Ref. [22].

when x_F further increases. A comparison between Fig. 1 and Fig. 2(a) shows a striking similarity. Since the fall-off at large x_1 in the K^-/π^- Drell-Yan cross section ratio is described as a soft $U_K(x)$ distribution, it is conceivable that the pronounced drop of the K^-/π^- ratio at large x_F in Fig. 2(a) has a similar origin.

The NA3 collaboration has also measured the K^+/π^+ ratios for J/ψ production at 200 GeV on a platinum target as shown in Fig. 2(b) [45]. A significant difference between the K^+/π^+ and the K^-/π^- ratios is observed. While there is a pronounced drop of the K^-/π^- ratio at forward x_F, no such drop is present for K^+/π^+. Moreover, Figs. 2(a) and 2(b) show that the K^+/π^+ ratios are $\sim$ 20% lower than for the K^-/π^- ratio.

The only other J/ψ production data with kaon beams were obtained by the WA39 collaboration using 39.5 GeV beam on a tungsten target [46]. Both the K^-/π^- and the K^+/π^+ J/ψ cross section ratios were measured, as shown in Fig. 2(c) and Fig. 2(d). The K^+/π^+ ratios at 39.5 GeV are notably lower than that at 200 GeV. These K/π J/ψ production data, together with the K^-/π^- Drell-Yan data, are utilized in this analysis for the first determination of the kaon PDFs. The striking energy dependence of the K^+/π^+ J/ψ ratios, as well as the difference between the K^-/π^- and K^+/π^+ J/ψ ratios, suggests the possibility of flavor separation, namely, to distinguish the quark and gluon distributions in kaon, as discussed later.

For the calculation of the J/ψ production cross section, we adopt the non-relativistic QCD (NRQCD) [47] approach. The NRQCD framework, which was also used in the recent analysis of the pion-induced J/ψ production data to extract the pion PDFs [32], is based on the factorization of the heavy-quark $Q\bar{Q}$ pair production and its subsequent hadronization. The production of the $Q\bar{Q}$ pair involves short-distance partonic interaction, calculated using perturbative QCD. The subprocesses include the gluon-gluon fusion, quark-antiquark annihilation, and quark-gluon interaction.

In NRQCD the probability of a $Q\bar{Q}$ pair hadronizing into a quarkonium bound state is described by the long-distance matrix elements (LDMEs). The LDMEs, assumed to be universal and independent of the beam type, are determined from the experimental data [48]. The LDMEs used in the NRQCD calculation were taken from a recent study [14], which extracts these matrix elements by performing a global fit to the J/ψ production cross sections induced by proton and pion beams at fixed-target energies. Several sets of the LDMEs were obtained in this work [14] and we have selected the "Fit-2" solution. We found that the results of the present analysis are insensitive to the choice of the specific LDME set.

Since the available Drell-Yan and J/ψ data used in this analysis are all in the form of the K/π cross section ratios, both the pion and the kaon PDFs are needed for the calculation. As the pion PDFs were already extracted in the framework of the statistical model, we fix the pion PDFs according to the results obtained from this recent study [32] while allowing the kaon PDFs to vary. The best-fit values for the various parameters in the statistical model are obtained for kaon. Table 1 lists the number of data points and the values of χ^2 for the best fit to the various data. In the global fit, the normalizations for various data sets are allowed to vary, i.e., the result of the calculated K/π ratio is multiplied by a K factor when compared with the data. We find that the K factors for the fit to Drell-Yan and J/ψ data are very close to 1 for negative mesons, and the K factors for positive mesons are within 18% of unity, consistent with the normalization uncertainties of the experiments.

Table 1
Values of the K factor χ^2 for each data set obtained from a global fit. P is the beam momentum, K the factor to be multiplied to the calculated Drell-Yan and J/ψ cross section ratios, and ndp the number of data points.

Experiment	P (GeV)	K	ndp	χ^2	χ^2/ndp
K^-/π^- DY NA3	150	1.052	8	4.05	0.51
$K^-/\pi^- J/\psi$ WA39	39.5	0.98	8	3.7	0.45
$K^-/\pi^- J/\psi$ NA3	150	1.028	19	21.2	1.12
$K^+/\pi^+ J/\psi$ WA39	39.5	1.15	7	4.0	0.58
$K^+/\pi^+ J/\psi$ NA3	200	1.18	17	11.0	0.65
Total			59	43.95	0.74

The small χ^2/ndp values listed in Table 1 show that a satisfactory description of the Drell-Yan and J/ψ K/π data can be achieved in the statistical model. This is also shown in Fig. 1 and Fig. 2, where the K/π data for the Drell-Yan and the J/ψ production are compared with the calculations. To illustrate the importance of including the J/ψ data in extracting the kaon PDFs, the dashed curves in Fig. 2 show the NRQCD calculation using the kaon and pion PDFs obtained in the maximum entropy approach [22]. The poor agreement with the data suggests that the sparse Drell-Yan data alone are not sufficient to determine the kaon PDFs.

The best-fit parameters of the kaon PDFs, obtained at an initial scale $Q_0^2 = 1$ GeV^2, are:

$$\begin{aligned}
A_{UK} &= 1.12 \pm 0.05 & b_{UK} &= 0.602 \pm 0.017 \\
X_{UK} &= 0.688 \pm 0.01 & \bar{x} &= 0.109 \pm 0.001 \\
\tilde{A}_{UK} &= 4.83 \pm 0.74 & \tilde{b}_{UK} &= 1.248 \pm 0.05 \\
A_{SK} &= 1.14 \pm 0.02 & b_{SK} &= 0.73 \pm 0.009 \\
X_{SK} &= 0.784 \pm 0.01 & A_{GK} &= 108.97 \pm 1.0\,. \qquad (6)
\end{aligned}$$

The uncertainties of the parameters in Eq. (6) are statistical only. The K/π cross section ratios are not sensitive to the uncertainty of the nuclear PDFs. To evaluate the impact of the uncertainty of the pion PDFs on the extracted kaon PDFs, a future analysis to fit simultaneously the pion and kaon data is anticipated. The temperature, $\bar{x} = 0.109$, found for kaon is very close to that obtained for pion, $\bar{x} = 0.119$ [32], indicating a common feature for the statistical description for pion and kaon. On the other hand, the chemical potential for the valence quark of pion, $X_U = 0.72$, is between the corresponding chemical potentials of $X_{UK} = 0.688$ and $X_{SK} = 0.784$ for kaon. The global fit to the existing meson-induced Drell-Yan and J/ψ production data in the statistical model naturally leads to the result, $X_{SK} > X_U > X_{UK}$. The smaller chemical potential for $\bar{u}$ in K^- than $\bar{u}$ in π^- accounts for a softer x distribution for $U_K(x)$ than $U_\pi(x)$, resulting in the drop of the K^-/π^- ratios at the large $x_1(x_F)$ region for both the Drell-Yan and the J/ψ production data. Fig. 3(a) displays the valence quark distributions at $Q^2 = 10$ GeV^2 for kaon and pion obtained in the statistical mode analysis. The hierarchy that $S_K(x)$ is harder than $U_\pi(x)$, together with $U_\pi(x)$ being harder than $U_K(x)$, is preserved at the J/ψ production scale of $Q^2 = 10$ GeV^2. The sea-quark and gluon distributions are shown in Fig. 3(b). The gluon distributions are found to be very similar for pion and kaon.

To obtain some insight on how the K^-/π^- and K^+/π^+ ratios for J/ψ production can constrain the kaon PDFs, we have examined the decomposition of the J/ψ production cross sections for kaon beam into the $q\bar{q}$ annihilation and the gg fusion processes. For K^- beam at 39.5 GeV, the $q\bar{q}$ annihilation is the dominant subprocess, while the gg fusion becomes more important at the higher energy of 150 GeV. Consequently, the combination of the J/ψ production data at the 39.5 and 150 GeV could constrain both the valence-quark and the gluon contents in kaon. For the K^+ beam, which contains the u and $\bar{s}$ valence quarks, the $q\bar{q}$ annihilation process is suppressed since a sea quark in the nucleon is required. Hence the gg fusion process is important for K^+ not only at 200 GeV but also at the lower beam energy of 39.5 GeV. Thus, the K^+/π^+ data at both beam energies are sensitive to the gluon distribution of kaon.

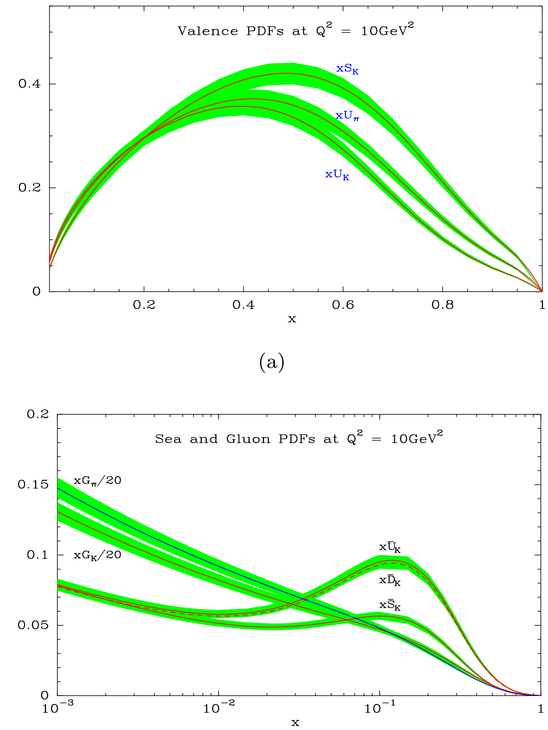

(a)

(b)

Fig. 3. Kaon PDFs obtained from a fit to the K/π ratios from Drell-Yan and J/ψ production experiments in the statistical model. (a): Valence quark distributions and (b): Sea-quark and gluon distributions. The pion quark and gluon distributions are also shown for comparison.

Table 2
Momentum fractions of valence quarks, sea quarks, and gluons for π^- and K^- at the scale $Q^2 = 10$ GeV^2 obtained in the statistical model.

	u Valence	d Valence	s Valence	all Sea	Gluon
π^-	0.242 ± 0.004	0.242 ± 0.004	–	0.188 ± 0.004	0.326 ± 0.015
K^-	0.220 ± 0.002	–	0.276 ± 0.001	0.162 ± 0.006	0.331 ± 0.018

Table 2 lists the momentum fractions carried by the valence quarks, sea quarks, and gluons in K^- obtained in this work at $Q^2 = 10$ GeV^2. The corresponding momentum fractions for π^- obtained in the statistical model analysis [32] are also shown for comparison. As discussed above, the softer x distribution for $\bar{u}$ valence quark in K^- leads to a smaller $\bar{u}$ momentum fraction in K^- than in π^-. Table 2 also shows that the momentum fraction carried by gluons in kaon is comparable to that in pion. This finding is at variance with the prediction of Ref. [18], but consistent with the expectation of Ref. [20]. As the gluon contents in the pion and kaon are better constrained when the J/ψ production data are included in the global analysis, this work provides the first evidence that the momentum fractions taken by the gluons are comparable for the pion and kaon.

In summary, we have performed an extraction of kaon's PDFs in the statistical model from a global fit to existing kaon-induced Drell-Yan and J/ψ production data. These data are well described by the statistical model approach. The inclusion of the K/π data for J/ψ production provides additional constraints on the valence as well as the gluon distributions of kaon. Both the Drell-Yan and J/ψ production data favor a harder valence distribution for strange quark than for up quark in kaon. A simultaneous fit to the K^-/π^- and K^+/π^+ J/ψ data allows a sensitive determination of the gluon distribution in the kaon, and the momentum fractions carried by gluon are found to be similar for pion and kaon. While the present analysis is performed in the framework of the statistical model, it would be interesting to extend this work using other different approaches for parametrizing the kaon PDFs. New kaon-induced Drell-Yan and J/ψ production data anticipated from AMBER [31] would provide further constraints on the kaon PDFs. In particular, a significantly improved precision of the AMBER data could lead to a determination of the most suitable functional forms for the kaon PDFs.

This work was supported in part by the U.S. National Science Foundation Grant No. PHY-1812377 and the National Science and Technology Council of Taiwan (R. O. C.).

Declaration of competing interest

The authors declare that they have no known competing financial interests or personal relationships that could have appeared to influence the work reported in this paper.

Data availability

Data will be made available on request.

References

[1] R. Holt, C.D. Roberts, Distribution functions of the nucleon and pion in the valence region, Rev. Mod. Phys. 82 (2010) 2991.
[2] S.D. Drell, T.M. Yan, Massive lepton pair production in hadron-hadron collisions at high-energies, Phys. Rev. Lett. 25 (1970) 316.
[3] H.B. Greenlee, et al., E326 Collaboration, Production of massive muon pairs in π^--nucleus collisions, Phys. Rev. Lett. 55 (1985) 1555.
[4] J.S. Conway, et al., E615 Collaboration, Experimental study of muon pairs produced by 252-GeV pions on tungsten, Phys. Rev. D 39 (1989) 92.
[5] B. Betev, et al., NA10 Collaboration, Differential cross-section of high-mass muon pairs produced by a 194 GeV/c π^- beam on a tungsten target, Z. Phys. C 28 (1985) 9.
[6] J.F. Owens, Q^2-dependent parametrizations of pion parton distribution functions, Phys. Rev. D 30 (1984) 943.
[7] P. Aurenche, R. Baier, M. Fontannaz, M.N. Kienzle-Focacci, M. Werlen, The gluon content of the pion from high p_T direct photon production, Phys. Lett. B 233 (1989) 517.
[8] M. Gluck, E. Reya, A. Vogt, Pionic parton distributions, Z. Phys. C 53 (1992) 651.
[9] P.J. Sutton, A.D. Martin, R.G. Roberts, W.J. Stirling, Parton distributions for the pion extracted from Drell-Yan and prompt photon experiments, Phys. Rev. D 45 (1992) 2349.
[10] P.C. Barry, N. Sato, W. Melnitchouk, C.R. Ji, First Monte Carlo global QCD analysis of pion parton distributions, Phys. Rev. Lett. 121 (2018) 152001.
[11] I. Novikov, et al., Parton distribution functions of the charged pion within the xFitter framework, Phys. Rev. D 102 (2020) 014040.
[12] J.C. Peng, W.C. Chang, S. Platchkov, T. Sawada, Valence quark and gluon distributions of kaon from J/ψ production, arXiv:1711.00839, 2017.
[13] W.C. Chang, J.C. Peng, S. Platchkov, T. Sawada, Constraining gluon density of pions at large x by pion-induced J/ψ production, Phys. Rev. D 102 (2020) 054024.
[14] C.Y. Hsieh, Y.S. Lian, W.C. Chang, J.C. Peng, S. Platchkov, T. Sawada, NRQCD analysis of charmonium production with pion and proton beams at fixed-target energies, Chin. J. Phys. 73 (2021) 13.
[15] W.C. Chang, J.C. Peng, S. Platchkov, T. Sawada, Fixed-target charmonium production and pion parton distributions, Phys. Rev. D 107 (2023) 056008.
[16] J. Badier, et al., Measurement of the K^-/π^- structure function ratio using the Drell-Yan process, Phys. Lett. B 93 (1980) 354.
[17] L. Chang, et al., Basic features of the pion valence-quark distribution function, Phys. Lett. B 737 (2014) 23.
[18] C. Chen, et al., Valence-quark distribution functions in the kaon and pion, Phys. Rev. D 93 (2016) 074021.
[19] P. Hutauruk, et al., Flavor dependence of the pion and kaon form factors and parton distribution functions, Phys. Rev. C 94 (2016) 035201.
[20] Z.F. Cui, et al., Kaon and pion parton distributions, Eur. Phys. J. 80 (2020) 1064.
[21] K.D. Bednar, I.C. Cloët, P.C. Tandy, Distinguishing quarks and gluons in pion and kaon parton distribution functions, Phys. Rev. Lett. 124, 042002.
[22] C. Han, G. Xie, X. Chen, An analysis of parton distribution functions of the pion and the kaon with the maximum entropy input, Eur. Phys. J. C 81 (2021) 302.
[23] X. Ji, Parton physics on a Euclidean lattice, Phys. Rev. Lett. 110 (2013) 262002; X. Ji, Y.S. Liu, Y. Liu, J.H. Zhang, Y. Zhao, Large-momentum effective theory, Rev. Mod. Phys. 93 (2021) 035005.
[24] J.H. Zhang, J.W. Chen, L. Jin, H.W. Lin, A. Schäfer, Y. Zhao, First direct lattice-QCD calculation of the x-dependence of the pion parton distribution function, Phys. Rev. D 100 (2019) 034505.
[25] R.S. Sufian, J. Karpie, C. Egerer, K. Orginos, J.W. Qiu, D.G. Richards, Pion valence quark distribution from matrix element calculated in lattice QCD, Phys. Rev. D 99 (2019) 074507.
[26] X. Gao, L. Jin, C. Kallidonis, N. Karthik, S. Mukherjee, P. Petreczky, C. Shugert, S. Syritsyn, Y. Zhao, Valence parton distribution of the pion from lattice QCD: approaching the continuum limit, Phys. Rev. D 102 (2020) 094513.
[27] Z. Fan, H.W. Lin, Gluon parton distribution of the pion from lattice QCD, Phys. Lett. B 823 (2021) 136778.
[28] H.W. Lin, J.W. Chen, Z. Fan, J.H. Zhang, R. Zhang, Valence-quark distribution of the kaon and pion from lattice QCD, Phys. Rev. D 103 (2021) 014516.
[29] C. Alexandrou, et al., Pion and kaon $\langle x^3 \rangle$ from lattice and PDF reconstruction from Mellin moments, Phys. Rev. D 104 (2022) 094510.
[30] A. Salas-Chavira, Z. Fan, H.W. Lin, Valence-quark distribution of the kaon and pion from lattice QCD, Phys. Rev. D 106 (2022) 094510.
[31] B. Adams, et al., Letter of intent: a new QCD facility at the M2 beam line of the CERN SPS (COMPASS++/AMBER), arXiv:1808.00848, 2018.
[32] C. Bourrely, W.C. Chang, J.C. Peng, Pion partonic distributions in a statistical model from pion-induced Drell-Yan and J/ψ production data, Phys. Rev. D 105 (2022) 076018.
[33] C. Bourrely, F. Buccella, J. Soffer, A statistical approach for polarized parton distributions, Eur. Phys. J. C 23 (2002) 487.
[34] C. Bourrely, F. Buccella, J. Soffer, The statistical parton distributions: status and prospects, Eur. Phys. J. C 41 (2005) 327.
[35] A. Baldit, et al., Study of the isospin symmetry breaking in the light quark sea of the nucleon from the Drell-Yan process, Phys. Lett. B 332 (1994) 244.
[36] R.S. Towell, et al., Improved measurement of the anti-d/anti-u asymmetry in the nucleon sea, Phys. Rev. D 64 (2001) 052002.
[37] J. Dove, et al., The asymmetry of antimatter in the proton, Nature 590 (2021) 561.
[38] J. Adam, et al., Measurement of the longitudinal spin asymmetries for weak boson production in proton-proton collisions at $\sqrt{s} = 510$ GeV, Phys. Rev. D 99 (2019) 051102.
[39] C. Bourrely, J. Soffer, New developments in the statistical approach of parton distributions: tests and predictions up to LHC energies, Nucl. Phys. A 941 (2015) 307.
[40] J.T. Londergan, J.C. Peng, A.W. Thomas, Charge symmetry at the partonic level, Rev. Mod. Phys. 82 (2010) 2009.
[41] C. Bourrely, J. Soffer, Statistical approach of pion parton distributions from Drell-Yan process, Nucl. Phys. A 981 (2019) 118.
[42] C.P. Salam, J. Rojo, A higher order perturbative parton evolution toolkit (HOPPET), Comput. Phys. Commun. 180 (2009) 120.
[43] F. James, M. Roos, CERN Program Library Long Writeup D506, 1994.
[44] C. Bourrely, F. Buccella, J.C. Peng, A new extraction of pion parton distributions in the statistical model, Phys. Lett. B 813 (2021) 136021.
[45] J. Badier, et al., Experimental J/ψ hadronic production from 150 to 280 GeV/c, Z. Phys. C 20 (1983) 101.
[46] M.J. Corden, et al., Experimental results on J/ψ production by $\pi^\pm, K^\pm, p$ and $\bar{p}$ beams at 39.5 GeV, Phys. Lett. B 96 (1980) 411.
[47] G.T. Bodwin, E. Braaten, G.P. Lepage, Rigorous QCD analysis of inclusive annihilation and production of heavy quarkonium, Phys. Rev. D 51 (1995) 1125; Phys. Rev. D 55 (1997) 5853(E).
[48] M. Beneke, I.Z. Rothstein, Hadroproduction of quarkonia in fixed target experiments, Phys. Rev. D 54 (1996) 2005; Phys. Rev. D 54 (1996) 7082(E).